EPJ Web of Conferences **95**, 04049 (2015)
DOI: 10.1051/epjconf/20159504049
© Owned by the authors, published by EDP Sciences, 2015

Results on neutrinoless double beta decay of ^{76}Ge from the GERDA experiment

Dimitrios Palioselitis[1,a] on behalf of the GERDA collaboration

[1] *Max-Planck-Institut für Physik, München, Germany*

Abstract. The Germanium Detector Array (GERDA) experiment is searching for neutrinoless double beta ($0\nu\beta\beta$) decay of ^{76}Ge, a lepton number violating nuclear process predicted by extensions of the Standard Model. GERDA is an array of bare germanium diodes immersed in liquid argon located at the Gran Sasso National Laboratory (LNGS) in Italy. The results of the GERDA Phase I data taking with a total exposure of 21.6 kg yr and a background index of 0.01 cts/(keV kg yr) are presented in this paper. No signal was observed and a lower limit of $T^{0\nu}_{1/2} > 2.1\times10^{25}$ yr (90% C.L.) was derived for the half-life of the $0\nu\beta\beta$ decay of ^{76}Ge. Phase II of the experiment aims to reduce the background around the region of interest by a factor of ten.

1 Introduction

For some even-even nuclei, decay via single β-emission is energetically forbidden. However, their neutrino accompanied double beta ($2\nu\beta\beta$) decay is allowed in the framework of the Standard Model. This decay is a second order weak process with very long half-life. It has been observed for several isotopes and the experimentally determined half-lives lie in the range of 10^{19} to 10^{24} years [1, 2].

The observation of neutrinoless double beta ($0\nu\beta\beta$) decay would imply lepton number violation by two units, indicating physics beyond the Standard Model of particle physics. Additionally, it would prove that neutrinos have a Majorana mass component. The half-life limits set so far on $0\nu\beta\beta$ decay for ^{76}Ge lie in the range of $(1.6-1.9)\times10^{25}$ years [3–5]. In 2004, a subgroup of the HdM collaboration claimed an observation of $0\nu\beta\beta$ decay [6], reporting a half-life of $T^{0\nu}_{1/2} = (1.19^{+0.37}_{-0.23})\times10^{25}$ years. The experimental signature of $0\nu\beta\beta$ decay is a peak at the Q-value of the decay, $Q_{\beta\beta} = 2039$ keV, which lies above the continuous energy spectrum of the $2\nu\beta\beta$ decay.

The GERDA experiment is introduced in section 2. In section 3, the results from GERDA Phase I are presented. The measurement of the half-life of $2\nu\beta\beta$ decay, the modelling of the background energy spectrum, the background discrimination methods and finally the result on the search of $0\nu\beta\beta$ decay are discussed. An outline of the ongoing transition to Phase II is given in section 4.

2 The GERDA experiment

The GERDA experiment searches for the $0\nu\beta\beta$ decay of ^{76}Ge [7]. The experiment is located at the Laboratori Nazionali del Gran Sasso (LNGS) in Italy. GERDA operates bare germanium diodes inside

[a] e-mail: dimitris@mpp.mpg.de

This is an Open Access article distributed under the terms of the Creative Commons Attribution License 4.0, which permits unrestricted use, distribution, and reproduction in any medium, provided the original work is properly cited.

Article available at http://www.epj-conferences.org or http://dx.doi.org/10.1051/epjconf/20159504049

liquid argon (LAr) which serves as a coolant and as shielding. The array of germanium detectors is inside a stainless steel cryostat filled with 64 m^3 of LAr. The cryostat is located inside a water tank that contains 590 m^3 of high purity water, moderating ambient neutrons and gamma radiation. The water tank is instrumented with 66 photomultiplier tubes (PMTs) and operates as a Čerenkov muon veto reducing cosmic induced background.

Eight p-type high purity germanium (HPGe) semi-coaxial detectors from the HdM [3] and IGEX [4] experiments were refurbished and used as the main GERDA Phase I detectors. They are enriched to ~86% in ^{76}Ge and have a total mass of 17 kg. Additionally, 30 enriched p-type broad energy germanium (BEGe) detectors were produced and will be used in Phase II of the experiment. Five of them, corresponding to a mass of 3.6 kg, were already deployed in GERDA during Phase I.

The data collected during Phase I, from November 2011 until May 2013, correspond to 492 days and a total exposure of 21.6 kg yr. The average duty cycle is 88%. The data were divided into three datasets. The *golden coaxial dataset* with an exposure of 17.9 kg yr contains all data taken with the enriched semi-coaxial detectors with the exception of a short period of approximately 30 days. This was due to increased activity after the insertion of the five BEGe detectors. This dataset, referred to as *silver coaxial dataset*, corresponds to 1.3 kg yr. The *BEGe dataset* consists of data taken with the BEGe detectors and has an exposure of 2.4 kg yr.

The energy scale of the individual detectors is determined with regular calibration runs, taken every one or two weeks, using a ^{228}Th source. The energy shift between successive calibrations is less than 1 keV at $Q_{\beta\beta}$. The mean exposure-weighted energy resolutions for the GERDA detectors are 4.8 ± 0.2 keV for the semi-coaxial detectors and 3.2 ± 0.2 keV for the BEGe detectors.

3 Results

3.1 Measurement of the $2\nu\beta\beta$ decay half-life

The measurement of the half-life of the neutrino accompanied double beta decay of ^{76}Ge by GERDA corresponds to 5.04 kg yr of exposure [8]. The observed spectrum in the energy range between 600 and 1800 keV is dominated by the double beta decay of ^{76}Ge. The signal-to-background ratio in this energy range is on average 4:1. A global model was fitted to the observed energy spectra above the ^{39}Ar background. The model contains the $2\nu\beta\beta$ decay of ^{76}Ge and three background contributions from ^{42}K, uniformly distributed in LAr, as well as ^{214}Bi and ^{40}K from close sources, whose presence is established by the observation of their characteristic gamma lines. Possible contributions from other background components were included in the systematic uncertainties. The spectral fit has 32 free parameters, the $2\nu\beta\beta$ half-life, the detector masses and enrichment fractions and the background contributions. The experimental energy spectrum together with the best fit model and the individual spectral contributions are shown in figure 1. The lower panel shows the ratio between experimental data and the prediction of the best fit model. The green, yellow and red regions are the smallest intervals containing 68%, 95% and 99.9% probability for the ratio, respectively, assuming the best fit parameters.

The measured half-life is $T^{2\nu}_{1/2} = (1.84^{+0.14}_{-0.10}) \times 10^{21}$ yr. This result is shown in figure 2, together with previous publications and two weighted averages. The value reported by GERDA is longer than the previous measurements. The trend to obtain higher values for more recent measurements is probably related to the improved signal-to-background ratio, which reduces the relevance of background modelling and subtraction.

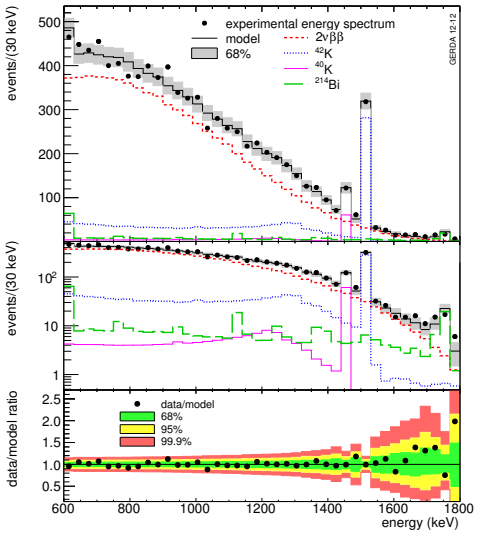

Figure 1. Upper and middle panels: experimental data (markers) and the best fit model (black histogram) in linear and logarithmic scale. Individual components are shown with coloured histograms. The shaded band covers the 68% probability range for the data, calculated from the expected counts of the best fit model. Lower panel: ratio between the experimental data and the best fit model, shown with the smallest intervals containing 68%, 95% and 99.9% probability for the ratio assuming the best fit parameters. Taken from [8].

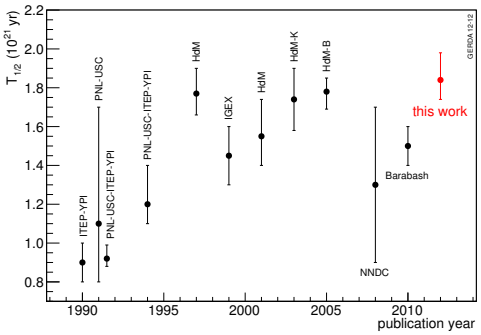

Figure 2. Experimental results for the half-life of the neutrino accompanied double beta decay, $T^{2\nu}_{1/2}$, of ^{76}Ge versus publication year. Taken from [8].

3.2 Background modelling

A background model was developed, prior to the $0\nu\beta\beta$ analysis, to describe the observed energy spectrum using data corresponding to an exposure of 18.5 kg yr [9]. The model contains several contributions that are either expected after material screening or established through the observation of characteristic structures in the energy spectrum. Figure 3 shows the energy spectra for the enriched semi-coaxial detectors, the BEGe detectors and one non-enriched detector. A 40 keV window around $Q_{\beta\beta}$ was kept blinded during the data taking and analysis. The low energy part, up to 565 keV, is dominated by the beta decay of cosmogenic ^{39}Ar. Between 600 and 1500 keV the spectra of the enriched detectors are dominated by the $2\nu\beta\beta$ decay. In all spectra, gamma lines from the decays of ^{40}K and ^{42}K can be identified. The spectra of the enriched semi-coaxial detectors also contain lines from ^{60}Co, ^{208}Tl, ^{214}Bi, ^{214}Pb and ^{228}Ac. A peak-like structure around 5.3 MeV in the spectrum of the enriched semi-coaxial detectors can be attributed to the decay of ^{210}Po on the detector p+ surfaces. Further peak-like structures at energies of 4.7, 5.4 and 5.9 MeV can be attributed to the alpha decays of ^{226}Ra, ^{222}Rn and ^{218}Po on the detector p+ surface, respectively.

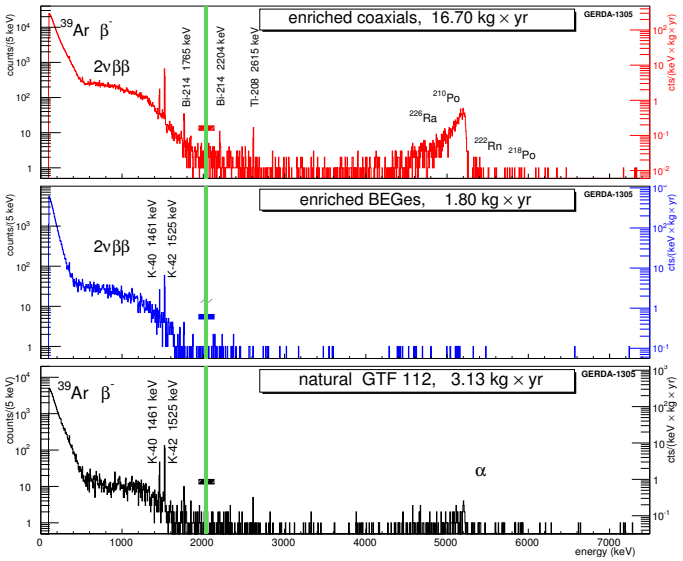

Figure 3. Energy spectra taken with all the enriched semi-coaxial (top), BEGe (middle) and non-enriched (bottom) detectors. The green band indicates the blinded region of 40 keV around $Q_{\beta\beta}$. The bars in the colour of the histogram around the blinded region indicate the 200 keV window used to determine the background index of each dataset. Taken from [9].

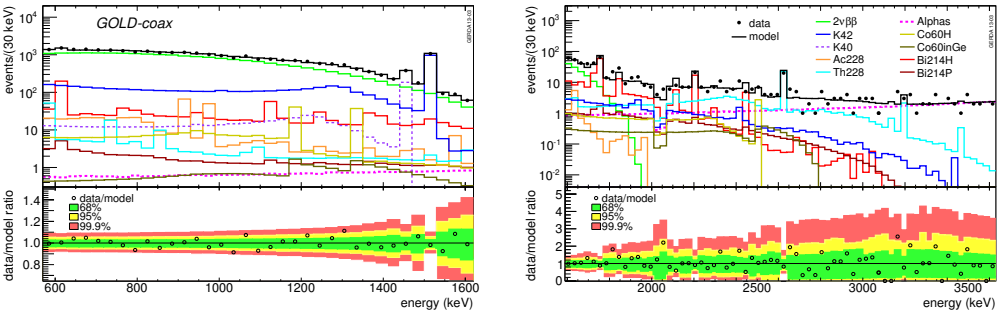

Figure 4: Experimental data (markers) and the best fit minimum model (black line) for the *golden coaxial dataset*. Individual background contributions are shown separately. The lower panels show the ratio between data and model, as well as the 68%, 95% and 99.9% probabilities for the ratios assuming the best fit parameters. Taken from [9].

The background model was obtained by fitting the simulated spectra of different contributions to the measured energy spectrum using a Bayesian approach. The high energy part of the spectrum between 3.5 and 7.5 MeV, above the Q-value of ^{42}K, was analysed first, providing a best fit for the alpha induced spectrum. This result was used along with other contributions to establish a model covering the energy range from 570 to 7500 keV. The main contributions at $Q_{\beta\beta}$ come from ^{42}K, ^{60}Co, ^{214}Bi, ^{208}Tl, as well as alpha events from surface contamination and ^{222}Rn in LAr. Figure 4 shows the best fit model in black, together with the observed counts and the individual background contributions considered in the fit, for the *golden coaxial dataset*. In the lower panels, the ratios of data and model are shown together with the smallest intervals of 68%, 95% and 99.9% probability for the model expectation.

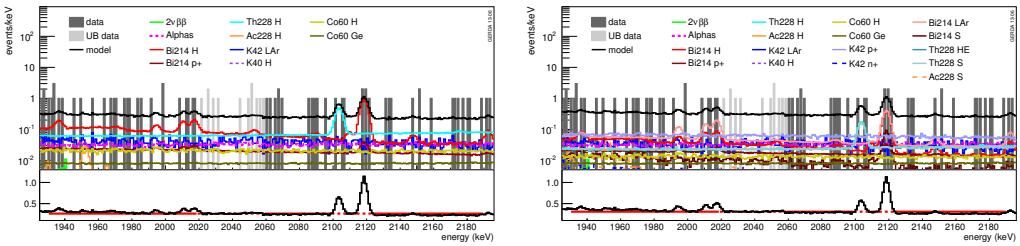

(a) (b)

Figure 5: Experimental spectrum with the minimum (a) and maximum (b) background model around $Q_{\beta\beta}$ for the *golden coaxial dataset*. The upper panels show the experimental data (grey histograms) with the individual background contributions considered in the fit (coloured histograms). The light grey histogram corresponds to the partially unblinded data, not used for the modelling of the background. The lower panels show the best fit models fitted with a constant. Taken from [9].

Two models were constructed for the background description, a minimal model consisting of well-motivated contributions (see figure 4) and a maximum model consisting of various additional contributions. They are shown in figure 5 together with the experimentally observed counts for the *golden coaxial dataset*. Both models show a good agreement with the data and their p-values do not favour one model over the other.

In order to confirm the validity of the background model, a partial unblinding took place. Only a small window of 10 keV for the semi-coaxial detectors and 8 keV for the BEGe detectors around $Q_{\beta\beta}$ remained blinded for the $0\nu\beta\beta$ analysis. The partially unblinded data are shown in light grey in figure 5. The agreement of the model with the data after the partial unblinding is satisfactory. One significant conclusion is that the spectrum between 1930 and 2190 keV can be modelled with a flat background, shown in the lower panels of figure 5. The background index at the region of interest is $(17.6 - 23.8) \times 10^{-3}$ cts/keV kg yr before applying any pulse shape discrimination algorithms.

3.3 Pulse shape analysis

The experimental sensitivity can be improved by analysing the pulse shapes of the detector signals with the aim of rejecting background events. Pulse shape discrimination (PSD) is therefore used to separate single-site (SSE) from multi-site (MSE) events. The signature of a double beta decay is a SSE, i.e. the energy is deposited locally in the detector. On the other hand, MSEs, e.g. from multiple Compton scattering, deposit energy in well separated locations in the detector.

Different PSD techniques were used for the semi-coaxial and the BEGe detectors [10]. This is due to the different geometries and, hence, different electric field distributions of the detectors. For the semi-coaxial detectors a neural network approach was utilised. The rising part of the charge pulse was used for the network analysis. For the BEGe detectors a mono-parametric A/E method was implemented, where A corresponds to the maximum of the current pulse and E is the reconstructed energy. For MSEs, the current pulses of the charges from different locations will have different drift times and, hence, more time-separated current pulses. Therefore, for the same total energy, E, the maximum amplitude, A, will be smaller for MSEs. For both methods, double-escape peak (DEP) events of 1593 keV serve as proxy of SSEs, while events in the full energy line of ^{212}Bi at 1621 keV are mostly MSEs and are used as the background sample.

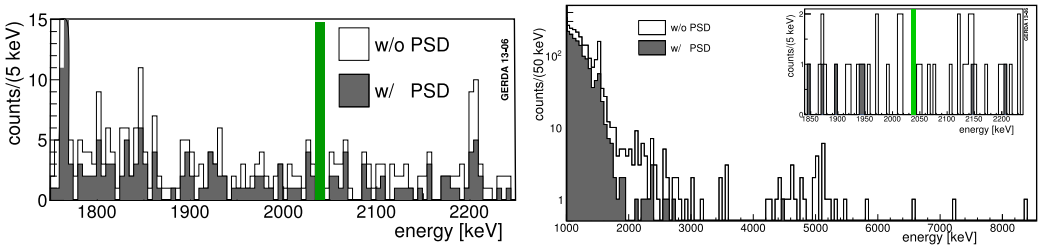

(a) (b)

Figure 6: Energy spectrum of the semi-coaxial (a) and BEGe (b) detectors with (filled histogram) and without (open histogram) PSD selection. The blinded window is indicated with a green band. Taken from [10].

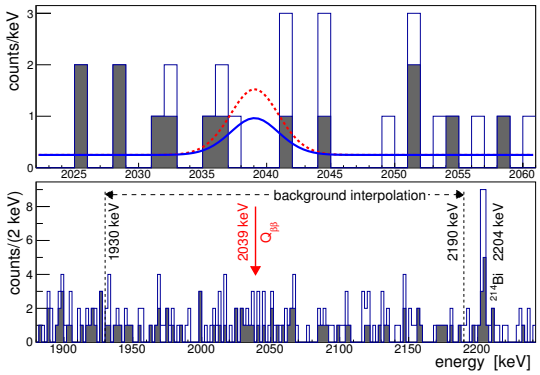

Figure 7. Energy spectrum around $Q_{\beta\beta}$ for all enriched germanium detectors with (filled) and without (open) PSD. The red dashed line corresponds to the expectation from [6] and the blue solid line is the 90% C.L. upper limit derived from the GERDA $0\nu\beta\beta$ analysis. The lower panel shows the energy region used for the background interpolation. Taken from [11].

Figure 6 shows the result of the PSD methods applied to data for the semi-coaxial and the BEGe detectors. The events surviving the PSD selection are shown in grey. The neural network method has a $0\nu\beta\beta$ acceptance of 90% while it rejects approximately half of the background around $Q_{\beta\beta}$. The A/E method has an efficiency of 92% and rejects 80% of the background events around $Q_{\beta\beta}$. On $2\nu\beta\beta$ events, the methods have an efficiency of 85% and 91% for the semi-coaxial and BEGe detectors, respectively.

3.4 Results on neutrinoless double beta decay

The combined energy spectrum from all enriched germanium detectors around the region of interest after unblinding is shown in figure 7. The filled histogram shows the counts after the PSD selection. In the lower panel, the energy region used for the background interpolation is shown.

After opening the blinded window, no excess of events was found above the expected background. Two analyses were performed to derive the lower limit for the half-life of $0\nu\beta\beta$ of ^{76}Ge. The baseline analysis was a frequentist analysis, where a profile likelihood fit was performed to the datasets using a common half-life. The best fit corresponded to zero counts and an upper limit of 3.5 counts. The derived lower limit for the half-life of $0\nu\beta\beta$ is $T^{0\nu}_{1/2} > 2.1 \times 10^{25}$ yr at 90% confidence level, including the systematic uncertainty. The corresponding median sensitivity for the 90% C.L. limit is $T^{0\nu}_{1/2} > 2.4 \times 10^{25}$ yr. A second Bayesian analysis was performed, using a flat prior on the inverse half-life

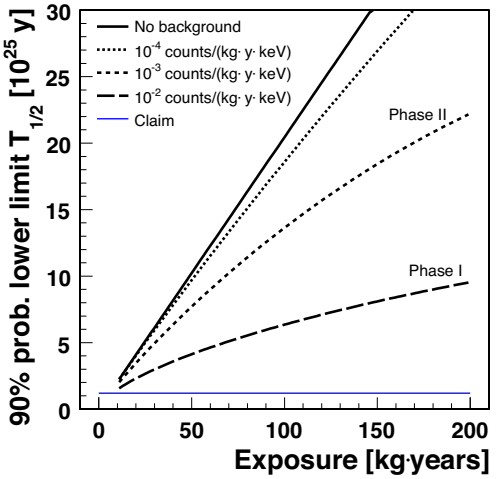

Figure 8. Sensitivity as a function of the exposure for different background cases. The lines corresponding to the background index of Phase I and Phase II are indicated on the figure. Taken from [12].

in the $0 - 10^{-24}\,\mathrm{yr}^{-1}$ range. The best fit was again zero counts corresponding to a lower limit of $T^{0\nu}_{1/2} > 1.9 \times 10^{25}$ yr at 90% credible interval. The median sensitivity is $T^{0\nu}_{1/2} > 2.0 \times 10^{25}$ yr. A combination of the GERDA result with the results from IGEX and HdM experiments gave a lower limit of $T^{0\nu}_{1/2} > 3.0 \times 10^{25}$ yr at 90% confidence level. In this case the profile likelihood fit was extended to include the energy spectra from the other two experiments. Constant background for all five datasets and gaussian peaks with a common half-life were assumed.

In order to compare the GERDA result with the signal claim, a hypothesis test was performed. The expected number of counts for the background only hypothesis, H_0, is 2 ± 0.3. As an alternative hypothesis, H_1, the claimed signal corresponding to a half-life of $T^{0\nu}_{1/2} = 1.19 \times 10^{25}$ yr plus a background was considered, corresponding to 5.9 ± 1.4 expected counts. In figure 7, the exposure corrected expectation according to the signal claim is shown in dotted red line together with the lower limit derived from the GERDA analysis in blue. The number of observed counts is 3. Assuming the model H_1, the probability to obtain zero counts as the best fit from the profile likelihood analysis is 0.01. Also the Bayes factor, i.e. the ratio of the probabilities of the two models $P(H_1)/P(H_0)$, computed with the GERDA result alone as well as with the combined result is 0.024 and 2×10^{-4}, respectively, therefore the claim is strongly disfavoured.

4 GERDA Phase II

In Phase II, GERDA aims to improve the half-life sensitivity by another order of magnitude. Figure 8 shows the sensitivity as a function of the exposure for different background levels. An order of magnitude improvement on the $0\nu\beta\beta$ half-life sensitivity is expected in approximately 5 years.

The twin lock system of Phase I was replaced by a new, single and larger lock system and the size of the detector array is increased to 7 strings. Both the detector array and the liquid argon instrumentation surrounding the array will be lowered into the cryostat under dry nitrogen atmosphere. The new cable chain is made of selected stainless steel of low radioactivity and cables that exhibit lower ^{228}Th and ^{226}Ra activities compared to Phase I cables, by more than a factor of 10.

The liquid argon instrumentation will be used as a scintillation background veto system. PMT arrays will be installed above and below the detector array. Silicon photomultipliers coupled to wavelength shifting fibres will surround the detector array. They will serve to detect scintillation light in

liquid argon, providing increased background reduction capability. Pulse shape analysis in combination with the liquid argon veto provide a suppression factor of 5.2×10^3 at $Q_{\beta\beta}$ for a close ^{228}Th source.

For Phase II, 30 new BEGe detectors were produced. For the detector modules, a significant amount of copper and PTFE has been replaced by intrinsically radio pure silicon. The energy resolution of these detectors was determined with a ^{60}Co source, in vacuum tests, to be less than 1.9 keV at 1.3 MeV. In addition, the PSD method of A/E, described in section 3.3, is a robust, simple and well-understood method of background rejection that was successfully implemented during Phase I. Finally, careful handling of the detectors during manufacturing and transportation insures a very low background contribution from ^{60}Co and ^{68}Ge due to cosmogenic activation.

5 Conclusions

The design goals of GERDA Phase I were reached. A total exposure of 21.6 kg yr was accumulated. The background index at $Q_{\beta\beta}$ after the application of PSD methods was 0.01 cts/keV kg yr. A blinded analysis looking for the $0\nu\beta\beta$ decay of ^{76}Ge was performed. No signal was observed and the most competitive limit on the half-life of this process for ^{76}Ge was derived, strongly disfavouring the long standing claim of $0\nu\beta\beta$ signal observation.

The transition to GERDA Phase II is ongoing. An additional 20 kg of detector mass will be deployed. The new custom-made BEGe detectors have an excellent PSD capability and a subset of them was tested successfully during Phase I. A liquid argon instrumentation for further background reduction will be installed. The background target of GERDA Phase II is 10^{-3} cts/keV kg yr, which will allow the exploration of $0\nu\beta\beta$ half-life values in the 10^{26} yr range.

References

[1] A.S. Barabash, Phys. Rev. C **81**, 035501 (2010)
[2] V.I. Tretyak, Y.G. Zdesenko, Atomic Data and Nuclear Data Tables **80**, 83 (2002)
[3] H. Klapdor-Kleingrothaus et al. (Heidelberg-Moscow Collaboration), The European Physical Journal A - Hadrons and Nuclei **12**, 147 (2001)
[4] C.E. Aalseth et al. (IGEX Collaboration), Phys. Rev. D **65**, 092007 (2002)
[5] C.E. Aalseth et al. (IGEX Collaboration), Phys. Rev. D **70**, 078302 (2004)
[6] H. Klapdor-Kleingrothaus, I. Krivosheina, A. Dietz, O. Chkvorets, Physics Letters B **586**, 198 (2004)
[7] K.H. Ackermann et al. (GERDA Collaboration), The European Physical Journal C **73**, 2330 (2013)
[8] M. Agostini et al. (GERDA collaboration), Journal of Physics G: Nuclear and Particle Physics **40**, 035110 (2013)
[9] M. Agostini et al. (GERDA Collaboration), The European Physical Journal C **74**, 2764 (2014)
[10] M. Agostini et al. (GERDA Collaboration), The European Physical Journal C **73**, 2583 (2013)
[11] M. Agostini et al. (GERDA Collaboration), Phys. Rev. Lett. **111**, 122503 (2013)
[12] A. Caldwell, K. Kröninger, Phys. Rev. D **74**, 092003 (2006)